

Magnetic interfaces in Fe-based nanocrystalline alloys determined by Mössbauer spectrometry

A. Ślawska-Waniewska

Institute of Physics, Polish Academy of Sciences, Al. Lotników 32/46, 02-668 Warszawa, Poland

J. M. Grenèche

Laboratoire de Physique de l'Etat Condensé, UPRES A CNRS 6087, Université du Maine, F72085 Le Mans, Cedex 9, France

(Received 14 May 1997)

Mössbauer investigations of $\text{Fe}_{89}\text{Zr}_7\text{B}_4$ nanocrystalline material, performed over the temperature range 4.2–550 K and in applied magnetic fields, are presented and interpreted in terms of the crystalline, amorphous, and interfacial contributions. The results obtained indicate that the interfaces exhibit structural as well as spin disorder with the thermal evolution of the mean hyperfine field similar to that of the crystalline bcc-Fe phase. [S0163-1829(97)50338-9]

Nanocrystalline materials produced by the partial devitrification of amorphous alloys consist structurally of crystalline grains with a long-range order and the residual amorphous matrix that exhibits a short-range order. The grains are randomly oriented but their atomic structure is identical. The magnetic behavior of such nanocrystalline alloys is usually described taking into account these two phases. It seems however that in such mesoscopic system an additional structural component comprising atoms situated at the grain surfaces and/or in the interphase boundaries has to be considered since the atomic structure (the local atomic density and the coordination numbers) in the boundary regions is different from that of the bulk crystalline and amorphous counterparts. During the last decade, many experimental observations confirmed the appearance of new properties of the granular materials, composed of assemblies of particles or the grains dispersed in an insulating matrix, due to the crystal size effects. Mössbauer investigations of Fe-rich granular materials show the existence of two distinct components which are ascribed to the crystalline interior and the interfacial region.^{1–3} However, even in the materials prepared by the same method (e.g., in nanostructured Fe prepared by the gas condensation technique) the considerable differences in the relative magnitudes of the hyperfine fields of the two major components as well as their temperature dependences have been observed.^{1,2} The earlier papers report on the enhancement of the average hyperfine field at the surfaces of fine iron particles at low temperatures and simultaneously a stronger temperature dependence of the hyperfine fields at the surface than that in the interior.¹ To the contrary, the recent data show that over the applied temperature range (4.2–200 K) the temperature dependences of $\langle H_{\text{hf}} \rangle$ for both components are roughly parallel with smaller values of the surface hyperfine fields.²

In this paper the role of the interfaces is studied in Fe-Zr-B nanocrystalline alloy in which, contrary to conventional granular materials, α -Fe grains are embedded in a magnetic matrix. Moreover, the Curie temperature of the crystalline phase is much higher than that of the amorphous one, thus, depending on the temperature, the role of the matrix being either in the ferromagnetic or paramagnetic state can be investigated, in both cases for the very same assembly of

grains. It has recently been shown that in this kind of materials the basic symmetry loss at the crystalline grain-amorphous material interface leads to a surface magnetostriction.⁴ Besides that, the room-temperature Mössbauer investigations provided experimental evidence for the existence of a specific state of some of the Fe atoms which have been identified with a special grain boundary phase.⁵ In this paper the results and analysis of the Mössbauer effect study over a wide temperature range in $\text{Fe}_{89}\text{Zr}_7\text{B}_4$ nanocrystalline alloys are presented. Moreover, the results of measurements carried out in the external magnetic field are also shown. The data presented do not provide a detailed picture of the structure of boundary regions, but bring information about the basic topological and magnetic properties as well as allow to estimate an average width of the interfacial layer.

$\text{Fe}_{89}\text{Zr}_7\text{B}_4$ nanocrystalline alloy, obtained by the isothermal annealing of the amorphous ribbon at 540 °C for 1 h under vacuum, is composed of α -Fe grains (about 10 nm of diameter) embedded in a residual amorphous matrix.⁴ Static magnetic measurements allow to estimate that the Curie temperatures of the crystalline and amorphous phases are 1043 and 423 K, respectively, whereas the volume fraction of the crystalline phase is about 77%.

Mössbauer investigations of $\text{Fe}_{89}\text{Zr}_7\text{B}_4$ nanocrystalline alloy were carried out with a conventional constant acceleration spectrometer and a $^{57}\text{Co}(\text{Rh})$ source over the temperature range 4.2–550 K. Representative spectra, typical of low and high temperatures, are shown in Fig. 1. The spectra obtained exhibit a rather complex hyperfine structure and consist of at least two superimposed components: a sextet with sharp well-defined lines which can be attributed to bcc-Fe crystalline phase and a broad Zeeman pattern characteristic of topologically disordered materials which can roughly be ascribed to the residual amorphous phase. On warming, this broad component collapses progressively into the paramagnetic doublet. However, in addition to these two main components, an additional contribution which appears as a shoulder of the outermost lines attributed to the crystalline phase at lower fields is observed. The effect of the asymmetrical broadening of the outer lines is the best visible at elevated temperatures where the hyperfine fields of the amorphous component are largely reduced and well separated from those

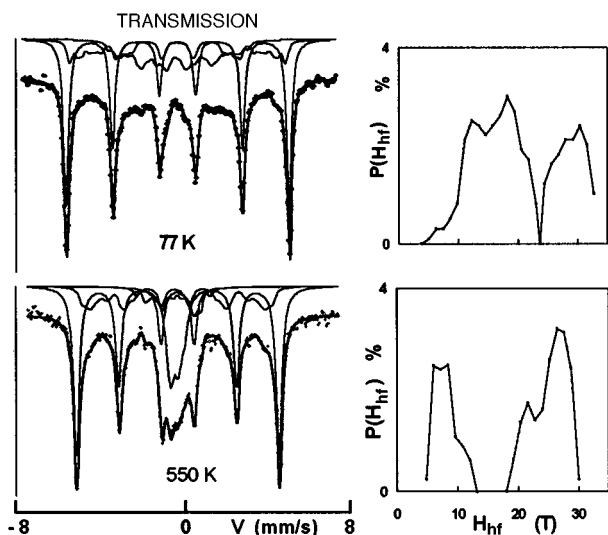


FIG. 1. Mössbauer spectra of $\text{Fe}_{89}\text{Zr}_7\text{B}_4$ nanocrystalline alloy and corresponding distributions of hyperfine fields.

of the crystalline one. Therefore, in the final fitting procedure the following contributions have been considered: (i) a sharp sextet with free hyperfine parameters, (ii) a component with a discrete distribution of the hyperfine fields in the low-field range (below ~ 20 T) which was linearly correlated to an isomer shift distribution and (iii) another component with a discrete distribution in the high hyperfine field range (~ 15 – 33 T) with the values of isomer and quadrupolar shifts similar to that obtained for the sharp magnetic sextet. At elevated temperatures, a quadrupolar component (iv) which appears in the central part of the spectra and which is attributed to the paramagnetic amorphous matrix, was also considered. It should be noted, however, that certain restrictions apply in the data analysis of such complex system, in particular arising from the relative strengths and correlations between the hyperfine interactions and the degree of overlap of spectral components. In the approach presented here the main problem consisted in the estimation of upper and lower limits of two broad distributions of hyperfine fields resulting from the contributions (ii) and (iii). Therefore, the spectra recorded at elevated temperatures, exhibiting better resolution between different components, were fitted first and relative amounts of Fe atoms in different regions have been estimated. Subsequently, Mössbauer spectra measured at lower temperatures have been fitted with the same procedure but taking into account the temperature evolution of different parameters and, simultaneously, preserving the numbers of Fe sites in each component (the value of f factor was assumed to be the same for all contributions). The detailed fits of selected spectra as well as the corresponding distributions of the hyperfine fields as shown in Fig. 1.

The temperature dependences of the hyperfine fields (H_{hf}), obtained for individual components of the Mössbauer spectra, are shown in Fig. 2. The upper curve a corresponds to the sharp sextet and reflects the temperature evolution of $H_{\text{hf}}^{\text{cr}}$ for the crystalline phase. The hyperfine parameters of this component are characteristic of the bulk iron and therefore it can unambiguously be identified with the interior of crystalline bcc-Fe grains. The lower curve c shows that the mean value of the hyperfine field ($H_{\text{hf}}^{\text{am}}$), fitted for the low-

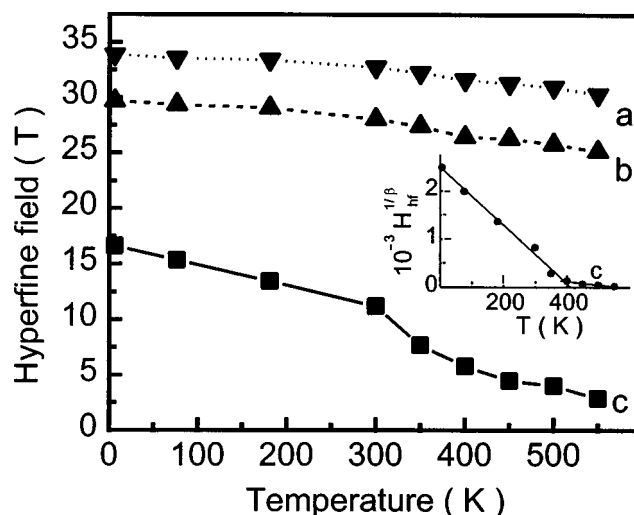


FIG. 2. Temperature dependence of mean hyperfine fields for bcc-Fe crystalline phase (a), interfaces (b) and amorphous matrix (c); the inset shows curve c in reduced coordinates.

field broad component, decreases with the increase of temperature up to about 400 K and remains small at higher temperatures. This component, characteristic of structurally disordered material, can be attributed to the residual amorphous phase. The temperature dependence of the average hyperfine field of this component can be easier analyzed when plotted, as shown in the inset in Fig. 2, in reduced coordinates $H_{\text{hf}}^{1/\beta}$ versus T (where $\beta=0.36$ is the empirical fit parameter). It is seen that this contribution can further be decomposed into two parts: (1) the main part originating from the amorphous matrix with the Curie temperature of about 420 K (in agreement with static magnetic measurements) and (2) an additional component, the relative contribution of which to the Mössbauer spectrum is below 2%, with the Curie temperature of about 550 K. Since this temperature corresponds well to the Curie point of Fe_3Zr crystals, it may indicate the presence of small amount (not noticeable by x-ray diffraction) of Fe_3Zr -like crystalline precipitates in the annealed sample. However, in the material with high fraction of the crystalline phase (like in the sample studied here), the small hyperfine fields may also be induced in the paramagnetic amorphous matrix by the strong exchange interactions between the grains which penetrate through the 1–2 nm thick paramagnetic spacer, as it was suggested by static magnetic measurements.⁶ The third sextet (iii), which appears in the high-field range (see Fig. 1), exhibits broad lines and the temperature dependence of its mean value of hyperfine field ($\langle H_{\text{hf}}^i \rangle$) is shown as curve b in Fig. 2. It is seen that the temperature evolution of $\langle H_{\text{hf}}^i \rangle$ of this additional subspectrum reflects the dependence obtained for the bcc phase but with the values about 10% lower than that for the bcc-Fe (curve a). Broad lines of this sextet as well as small (but nonzero) values of the quadrupolar shift indicate that it originates from the structurally disordered material whereas lower values of the hyperfine fields show that those of Fe atoms which have some nonmagnetic near neighbors contribute to this component. We attribute this extra component to the iron atoms located in boundary regions formed between crystalline grains and surrounded matrix.

The bimodal distributions of the hyperfine fields in

FeZrBCu nanocrystalline alloys have already been obtained from room-temperature Mössbauer spectra.^{7–9} The origin of the well-defined additional peak at the high-field side has not been discussed in Ref. 7 whereas Orue *et al.*⁸ attributed this peak to Fe-B crystalline phase (although any other experiments have not confirmed the existence of Fe-B crystalline precipitates). Kemény *et al.*⁹ observed again the extra subspectrum located at about 30 T (being satellite to the bcc-Fe contribution) and ascribed to Fe atoms in the bcc lattice which have Zr atoms in the nearest neighbor shell due to the peculiar properties of zirconium. However, the double-peak behavior of the hyperfine field distributions, with the mean field of the high field part at 29.5–30 T, have also been revealed in the alloys which do not contain Zr, e.g., in Fe-Nb-B.¹⁰ In this case this additional contribution was attributed to Fe atoms having some nonmagnetic near neighbors in the bcc lattice due to eventual dissolution of Nb and B in bcc grains. We note that the iron atoms in the grain, that are placed at the surface layer and are surrounded by the amorphous matrix, have the highest probability to have nonmagnetic neighbors. Moreover, since the coordination of Fe atoms at grain surfaces is lowered, whereas that of Fe atoms from the amorphous boundary region is enhanced, a wide spectrum of surface spin states can be created. These facts, together with the behavior of additional (high-field) component of the Mössbauer spectra, indicate that this extra sextet is attributed to Fe atoms placed at the interfaces formed at the crystalline grain-amorphous matrix boundaries. This conclusion can additionally be supported by the consideration of the relative contributions of different components to the Mössbauer spectrum. In the course of the fitting procedure it has been found that the volume fraction of the crystalline (i), amorphous (ii), and interfacial (iii) phases are $S_{cr}=56\%$, $S_{am}=23\%$ and $S_i=21\% \pm 2\%$, respectively. Considering that crystalline fraction, estimated from the bulk magnetization measurements (where at temperatures above the Curie point of the amorphous matrix, the grains together with the interfaces contribute to the saturation magnetization), is about 77%, a nice agreement with the Mössbauer data is obtained when the crystalline (i) and interfacial (iii) contributions are taken into account.

The thickness of the interface δ can be estimated from the relative contributions of different phases to the Mössbauer spectra in a simple geometrical model for spherical grains: $(S_{cr} + S_i)/S_{cr} = (1 + \delta/R)^3$, where R is the radius of the grain core with perfect crystalline structure. In the material studied $R=5$ nm, thus the width of the interfacial layer is $\delta \cong 0.6$ nm. In the real material, the grains are not so regular, thus this value is even overestimated indicating that the interface is formed by about 2 atomic layers.

The effect of the external magnetic field applied parallel to the direction of the incident γ rays (perpendicular to the ribbon plane) on the Mössbauer spectrum of the nanocrystalline Fe₈₉Zr₇B₄ alloy at 4.2 K is shown in Fig. 3. The zero-field spectrum shows that the magnetic moments of the grains are not randomly distributed but they are preferentially oriented within the ribbon plane (at about 70° from the normal to the ribbon plane) due to a very small effective anisotropy. Application of the external field of 10 kG perpendicular to the sample plane results in a decrease of the in-plane magnetization component and roughly random ori-

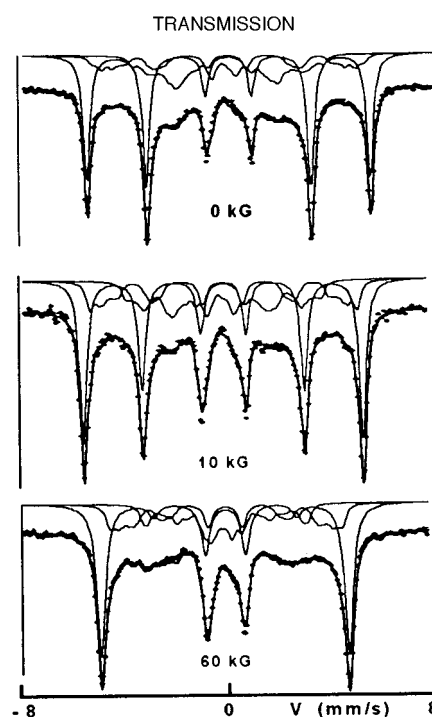


FIG. 3. Mössbauer spectra of Fe₈₉Zr₇B₄ nanocrystalline alloy at 4.2 K in zero field and in parallel field of 10 and 60 kG.

entation of magnetization in the grains. It is evident that 10 kG does not saturate the sample, the crystalline grains in particular. For stronger magnetic field (60 kG) the dominant response is the radical reduction of the second and fifth lines corresponding to the nuclear transition $\Delta I_z=0$ showing that the magnetic moments are preferentially oriented along the applied field. Moreover, the decrease of the total magnetic splitting is observed reflecting the negative sign of the effective field at the nucleus in ⁵⁷Fe (i.e., directed opposite to the direction of magnetization). The exemplary fits of the applied high-field spectrum are shown in Fig. 3. However, the detailed analysis of this spectrum cannot be performed due to the overlapped broad contributions of the spectral lines and the possible artifacts that can easily be created by the fitting procedure. The most reliable information that can be derived from this analysis is the amount by which the hyperfine field of the narrow component decreases with the applied field. In the field range 10–60 kG this decrease is of about 0.8 kG per one kG of the external field, which is a very reasonable value considering that at 10 kG the grains were not saturated in the field direction (this parameter is expected to be 1 for the saturated ferromagnet). From the spectra presented it is also evident that even in 60 kG the second and fifth lines do not completely disappear. Although it is very difficult to get a reliable separation for the individual components, nevertheless it is clear that at least in the topologically disordered regions, which in great part can be ascribed to the crystalline grain-amorphous matrix interfaces, the moments of Fe atoms are not collinear. One can consider two possible origins of the noncollinear spin arrangement of Fe atoms located in the interfaces. The first approach focuses on a wide distribution of the Fe-Fe nearest neighbor distances, typical of the structurally disordered interfacial layer, which can cause fluctuations in the magnitude and even changes in the sign of the

exchange interactions. Consequently, these competing ferromagnetic and antiferromagnetic interactions can lead to a noncollinear spin structure or a spin glasslike disorder of Fe spins, similar to that postulated for surface spins of various small magnetic particles (see, e.g., Refs. 11 and 12). The second explanation of the behavior of boundary regions observed in a strong magnetic field, could be a large surface/interface anisotropy arising from the magnetocrystalline, magnetoelastic and dipolar shape anisotropies.¹³ The surface magnetostriction, that is developing at the interfaces,⁴ is too small to be responsible for the observed effects. Moreover, it can be expected that the large interface anisotropy should pin the magnetic moment of the grain in a preferred orientation, which can change from grain to grain, and thus enhance the coercivity. It seems, however, that because of the soft magnetic behavior of these nanocrystalline ferromagnets, this explanation can be largely ruled out.

The results presented indicate that even if the grains are surrounded by a magnetic matrix, like in the material studied here, the spins at the grain surfaces and/or in the grain-matrix interfaces are canted. Although the crystalline and amorphous phases are coupled through the direct exchange interactions, this effect is not strong enough to prevent the noncollinear spin arrangements at the grain-matrix boundaries and to cover the phenomena related to finite-size effects in such a mesoscopic system.

In summary we have shown that in the nanocrystalline system the interfaces, formed at crystalline grain-amorphous matrix boundaries, do pose identifiable properties. The interfacial layer exhibits structural disorder with a distribution of

hyperfine fields in the range 22–35 T, and with a temperature dependence of the mean value of the hyperfine field similar to that of bcc-Fe phase. The important factor to note is that the magnetic behavior of the interfaces does not essentially depend on the magnetic properties of the matrix in which the grains are embedded. Even the ferro-paramagnetic phase transition of the amorphous matrix is hardly observable in the thermal evolution of the mean hyperfine field of the interfaces (see Fig. 3). The observed magnetic behavior of individual components indicates that the exchange interactions of Fe atoms situated in the interfaces with those in the crystalline interiors are responsible for the magnetic properties of the interfacial layer. The influence of the boundary regions does not noticeably extend into the crystalline interior (which behaves as a bulk iron). The observed behavior is expected considering that for transition metal alloys the electronic interactions which involve 3d electrons are of the short-range type (they are the strongest over one or two nearest neighbor shells). To the contrary, the range of a magnetic influence of the interface may be important for thin (1–2 nm) intergranular amorphous matrix, in particular it may be responsible for the weak magnetism observed at temperatures above its Curie point. The external magnetic field of 60 kG does not saturate the magnetic moments of Fe atoms in the interfacial regions indicating canting of the interfacial spins. It may be expected that, in addition to predominant ferromagnetic exchange interactions, small admixture of antiferromagnetically coupled Fe atoms occurs in the interfacial layer leading to its mixed magnetic behavior.

¹U. Herr, J. Jing, R. Birringer, U. Gonser, and H. Gleiter, *Appl. Phys. Lett.* **50**, 472 (1987).

²S. J. Campbell, J. Chadwick, R. J. Pollard, H. Gleiter, and U. Gonser, *Physica B* **205**, 72 (1995).

³Y. Sasaki, M. Hyakkai, Eiji Kita, A. Tasaki, H. Tanimoto, and Y. Iwamoto, *J. Appl. Phys.* **81**, 4736 (1997).

⁴A. Ślawska-Waniewska, R. Zuberek, and P. Nowicki, *J. Magn. Mater.* **157/158**, 147 (1996); A. Ślawska-Waniewska and J. Munoz, *ibid.* **160**, 251 (1996).

⁵A. Ślawska-Waniewska, K. Brzózka, and J. M. Greneche, *Acta Phys. Pol. A* **91**, 229 (1997).

⁶A. Ślawska-Waniewska, P. Nowicki, H. Lachowicz, P. Gorria, J. M. Barandiaran, and A. Hernando, *Phys. Rev. B* **50**, 6465 (1994).

⁷I. Navarro, A. Hernando, M. Vazquez, and Seon-Cho Yu, *J. Magn. Mater.* **145**, 313 (1995).

⁸I. Orúe, P. Gorria, F. Plazaola, M. L. Fernández-Gubieda, and J. M. Barandiarán, *Hyperfine Interact.* **94**, 2199 (1994).

⁹T. Kemény, L. K. Varga, L. F. Kiss, J. Balogh, A. Lovas, I. Vincze, and L. Toth, *Mater. Sci. Eng. A* (to be published).

¹⁰K. Suzuki, J. M. Cadogan, V. Sahajwalla, A. Inoue, and T. Masumoto, *Mater. Sci. Forum* **225–227**, 707 (1996).

¹¹A. H. Morrish, in *Studies of Magnetic Properties of Fine Particles*, edited by J. L. Dormann and D. Fiorani (Elsevier, New York, 1992), p. 181.

¹²R. H. Kodama, A. E. Berkowitz, S. Foner, and E. McNiff, *Mater. Sci. Forum* **235–238**, 643 (1997), and references therein.

¹³P. Bruno and J. P. Renard, *Appl. Phys. A* **49**, 499 (1989).